

Reduction of inward momentum flux by damped eigenmodes

P. W. Terry, D. A. Baver,^{a)} and D. R. Hatch

Department of Physics, University of Wisconsin–Madison, Madison, Wisconsin 53706, USA

(Received 25 August 2009; accepted 12 November 2009; published online 7 December 2009)

The inward momentum flux driven by the off-diagonal pressure gradient in a fluid model for ion temperature gradient turbulence with large Richardson number is significantly reduced by the excitation of stable eigenmodes. This is accomplished primarily through the amplitude autocorrelation of the damped eigenmode, which, in the flux, directly counteracts the quasilinear contribution of the unstable eigenmode. Stable eigenmode cross correlations also contribute to the flux, but the symmetry of conjugate pairing of growing and damped eigenmodes leads to significant cancellations between cross correlation terms. Conjugate symmetry is a property of unstable wavenumbers but applies to the whole of the saturated state because damped eigenmodes in the unstable range prevent the spread of energy outside that range. The heat and momentum fluxes are nearly isomorphous when expressed in terms of the eigenmode correlations. Due to this similarity of form, the thermodynamic constraint, which keeps the heat flux outward even when significantly reduced by the damped eigenmode, results in a momentum flux that remains inward, even though it is also reduced by the damped eigenmode. The isomorphism is not perfect. When the contribution of stable eigenmode cross correlations to the flux do not cancel, the momentum flux can reverse sign and become outward. © 2009 American Institute of Physics. [doi:10.1063/1.3271158]

I. INTRODUCTION

Momentum transport has emerged as a key issue for fusion plasmas because of its role in the formation of sheared flows and the effect of the latter on energy confinement.¹ Of considerable interest is the phenomenon of spontaneous or intrinsic rotation, which spins up a plasma in the absence of external momentum input.^{2–4} A leading hypothesis for intrinsic rotation is that momentum conservation is broken in the edge by some dissipative, nonambipolar, or symmetry-breaking process, creating a net rotation, and that inward transport then carries the momentum into the plasma core. Inward momentum transport mechanisms have been identified in turbulence theories^{5,6} and have been observed experimentally.^{7,8} The ion temperature gradient (ITG) instability in the presence of weak flow shear⁹ gives a momentum flux that is driven by the dominant pressure gradient. As an off-diagonal transport effect the momentum is carried up the pressure gradient, analogous to particle pinches.¹⁰ This effect is predicted by straightforward calculations using the quasilinear transport approximation.

This paper follows a different thread from other recent studies of anomalous momentum transport. It examines the effect on transport of nonlinearly excited eigenmodes that are linearly stable for all wavenumbers, addressing a trio of unanswered questions. These questions deal with the effect of damped eigenmodes on momentum transport in ITG turbulence, the way damped eigenmodes link different transport channels (in this case heat and momentum), and the way wavenumber variations in growth rate and frequency in both the unstable and damped-eigenmode branches affect saturation and transport. From previous work it is known that

stable eigenmodes affect both the magnitudes, cross phases, and scalings of heat and particle fluxes.^{11–13} For ITG, important deviations of the heat flux from the quasilinear value have been reported for both a simple reduced model¹² and comprehensive gyrokinetic models.¹³ The nonlinear effects behind these observations are of interest not just for their action on transport fluxes. They are symptomatic of saturation physics based on transfer to damped eigenmodes in the wavenumber range of the instability instead of a cascade to collisionally dissipated scales at large wavenumber. Damped eigenmodes are excited by mode coupling with unstable modes.¹²

Previous studies showed how damped eigenmodes reduce diagonal fluxes. Their effect on off-diagonal fluxes has not been considered. For example, in pressure-gradient-driven ITG turbulence with weak flow gradient, does the off-diagonal momentum flux behave like the diagonal heat flux? The latter is primarily reduced by the negative-definite (or inward transporting) contribution of the damped-eigenmode amplitude autocorrelation. Thermodynamic considerations dictate that this contribution not exceed the outward quasilinear contribution arising from the unstable eigenmode. Can the momentum flux, which is off diagonal, change sign, or does it simply show a reduction? To fully answer questions such as these one must consider eigenmode cross correlations, which also contribute to fluxes. Unlike the autocorrelations, their contribution to fluxes is not positive or negative definite. Eigenmode cross correlations are familiar in inertial magnetohydrodynamic turbulence where they describe the interaction of counterpropagating Alfvén wave packets but are unfamiliar in instability-driven microturbulence. In transport, eigenmode cross correlations are especially unfamiliar. One approach for understanding the role of cross correlations is to track the interrelationship of growth

^{a)}Present address: Lodestar Research Corp., Boulder, Colorado 80301.

rate and frequency spectra in both the unstable and damped-eigenmode branches and to determine how such relationships affect excitation, saturation, and transport. The symmetries of the ITG instability, which involve conjugate modes, introduce helpful simplifications into this problem.

Stable eigenmodes are normal-mode solutions of the Fourier-transformed linearized dynamical equations whose normal-mode frequency has an imaginary part that is zero or negative for all wavenumbers k . In an initial value problem, if such eigenmodes are part of the initial condition, they decay exponentially at their linear damping rate as long as nonlinearities are negligible. Unstable eigenmodes grow exponentially. The growth rates of unstable eigenmodes are generally positive only in some wavenumber range. At high k , collisional dissipation makes the growth rate negative. With growth at low k and damping at high k , it has been customary to assume that the concept of the hydrodynamic cascade applies to the unstable eigenmode as a means for saturating the instability. In Navier–Stokes turbulence and single-field models of plasma turbulence such as the Hasegawa–Mima equation,¹⁴ it is the only way to achieve a stationary state because the sole energy sink is collisional dissipation at high k . In plasma turbulence for any model with more than one fluid equation or for any kinetic model, there is at least one other eigenmode, and in all but the simplest models there are many eigenmodes. Typically these are damped for wavenumbers in the same range as the instability.

The nonlinear excitation of damped eigenmodes by mode coupling with the unstable eigenmode can easily be the dominant saturation path. A single three-wave interaction involving a damped eigenmode in the instability range provides prompt access to sinks without the need to excite many intermediate wavenumbers before reaching dissipated scales as in a cascade. This point highlights a crucial distinction between zonal flows, which are a type of damped eigenmode, and the kind of damped eigenmode just described, which saturates turbulence through a significant sink of fluctuation energy in the wavenumber range of the instability. Zonal flows with Hinton–Rosenbluth residual damping¹⁵ are weakly damped in many regimes, especially those with weak collisionality. They are therefore envisaged to regulate turbulence through the shearing mechanism. Shearing is an inertial effect that cannot directly dissipate energy but rather enhances the usual cascade to high- k dissipated wavenumbers.¹ On the other hand, damped eigenmodes that are not zonal flows and whose damping in the region of instability is of order the growth rate saturate the instability by absorbing its energy before it reaches high k . Consequently, turbulence regulation is not exclusive to zonal flows but can be accomplished by damped eigenmodes even without zonal flows. As with zonal flows, damped eigenmodes with $k_y=0$ play an important role in energy transfer dynamics.^{16,17} However, spectral transfer also excites damped eigenmodes with $k_y \neq 0$. The kind of direct contribution to transport fluxes described here is only possible for modes with $k_y \neq 0$.

Saturation by stable eigenmodes excited in the wavenumber range of the instability appears to be common in fluid models of plasma turbulence. It has previously

been identified in nearly a dozen systems applying to both tokamak core and edge, with fluctuations that range from ion scale to electron scale, and are electrostatic or electromagnetic.^{18,19} Saturation by damped eigenmodes has been inferred indirectly in gyrokinetics,¹³ and recent projections of stationary solutions of ITG turbulence onto the eigenmode basis now explicitly confirm that a very large number of damped eigenmodes are excited to large amplitude.²⁰ Provided there is at least one damped eigenmode whose damping rate is not significantly larger than the instability growth rate, the mechanism operates regardless of the details of the damped-eigenmode spectrum.¹² Systems in which the unstable mode is paired with a complex-conjugate or nearly complex-conjugate damped mode are of particular interest. These systems have both robust instability and robust damped-eigenmode activity. They also can be relatively simple if few eigenmodes are present in part because of the symmetry imparted by the conjugate pairing and in part because of the limited number of eigenmodes. The system studied in this paper meets these criteria.

To examine the effects of damped eigenmodes on momentum transport, we employ a transformation known as the *eigenmode decomposition* and focus on the structure and symmetry properties of the nonlinearities and transport fluxes in this representation. The eigenmode decomposition is a transformation of the dynamical equations from the original fields to fields representing the amplitudes of the linear eigenmodes. The latter is an alternate complete basis for nonlinear dynamical evolution. Generally the basis of linear eigenmodes is not orthogonal. The eigenmode basis diagonalizes linear coupling while generally mixing the nonlinearities. The latter reflects the fact that each eigenmode is generally driven by all nonlinearities of the system. In the eigenmode decomposition it is possible to track the energy transfer from the instability to every eigenmode that is nonlinearly excited and determine its role on transport. When transport fluxes are written using the eigenmode decomposition, the correlations between fluctuating fields are expanded as correlations between the complex-valued eigenmode amplitudes. The single term corresponding to the autocorrelation of the most unstable eigenmode amplitude is the quasi-linear flux. Due to the nonorthogonality of the basis, there are terms that depend on eigenmode cross correlations, i.e., on correlations of one eigenmode with a second distinct eigenmode. These correlations are nonzero because the eigenmodes couple nonlinearly under three-wave mode coupling satisfying the usual wavenumber condition $k=k'+k''$.

We study the effect of damped eigenmodes on transport fluxes using a reduced fluid model for ITG turbulence that couples ion pressure, potential, and parallel ion flow.^{12,21} The mean parallel flow has a weak radial gradient corresponding to large Richardson number. The system drives heat and momentum transport related to gradients of pressure and parallel flow. This model will be discussed more fully below. Analytical theory and numerical solutions yield the following.

- (1) The pressure gradient drives instability in the large Richardson number regime, yielding outward heat and

inward momentum fluxes in quasilinear theory, as previously established.⁹ The nonlinear excitation of the damped eigenmode significantly reduces both fluxes. In the fluxes the reduction resides primarily in the term proportional to the amplitude autocorrelation of the damped eigenmode. This directly counteracts the quasilinear contribution of the unstable eigenmode. The autocorrelation of the marginal mode amplitude makes no contribution to either flux.

- (2) The cross correlation between unstable and stable eigenmodes does not contribute to either flux due to symmetry associated with the conjugate pairing of these eigenmodes. Cross correlations between the marginal mode and either the stable or the unstable modes do contribute to the fluxes. Numerical solutions of saturated turbulence show that these contributions cancel most of the time. The cancellation has its roots in the conjugate symmetry.
- (3) The conjugate symmetry affects the whole of the saturated state as described in point (2), even though it holds only in the wavenumber range of the instability. This is because the robust energy sinks associated with the damped eigenmode over the wavenumber range of the instability prevent spread of energy to large wavenumbers. At large wavenumbers all eigenmode branches are stable, and conjugate symmetry does not hold. However, the fluctuation energy in this range is negligible, as is its contribution to the flux.
- (4) The heat and momentum fluxes are nearly isomorphous when expressed in terms of the eigenmode correlations. The isomorphism includes terms proportional to the auto correlations of unstable and stable eigenmodes and the real part of the cross correlation terms. Due to this similarity of form, the thermodynamic constraint, which keeps the heat flux outward even when significantly reduced by the damped eigenmode, results in a momentum flux that remains inward, even though it is also reduced by the damped eigenmode.
- (5) The isomorphism is broken by terms proportional to the imaginary part of the cross correlations. When the cross correlation contributions to the flux do not cancel, the momentum flux can reverse sign and become outward.

This paper is organized as follows. Section II presents the model and its linear stability properties. It also describes symmetry properties of the saturated state that arise from the conjugate pairing of unstable and damped eigenmodes. The momentum fluxes in the eigenmode decomposition are derived in Sec. III. Section IV describes the eigenmode cross correlations, their symmetry properties, and their role on the fluxes. Conclusions are presented in Sec. V.

II. LINEAR INSTABILITY AND SATURATION

We study a reduced fluid model for ITG that couples ion pressure, potential, and parallel ion flow.^{12,21} The basic model is given by

$$(1+k^2)\frac{\partial\phi}{\partial t}-ik_yv_D\phi(\hat{\eta}k^2-1)+ik_zu_{\parallel} \\ =-\sum_{k'}(k'\times\hat{z}\cdot k)\phi_{k'}\phi_{k-k'}k'^2\equiv(1+k^2)N_{\phi}, \quad (1)$$

$$\frac{\partial u_{\parallel}}{\partial t}+i\frac{k_z}{\hat{R}_i}\phi+ik_zp=-\sum_{k'}(k'\times\hat{z}\cdot k)\phi_{k'}u_{\parallel k-k'}\equiv N_{u_{\parallel}}, \quad (2)$$

$$\frac{\partial p}{\partial t}+ik_yv_D\hat{\eta}\phi=-\sum_{k'}(k'\times\hat{z}\cdot k)\phi_{k'}p_{k-k'}\equiv N_p, \quad (3)$$

where $v_D\equiv(cT_e/eB)d(\ln n_0)/dx$ is the drift velocity, $\hat{\eta}=(1+\eta_i)/\tau$, $\eta_i=d(\ln T_i)/d(\ln n_0)$ is the ratio of temperature to density gradient scale lengths, $\tau\equiv T_e/T_i$ is the ratio of electron to ion temperature, $1/\hat{R}_i=1+1/R_i$ is an effective Richardson number, and R_i is the Richardson number, defined by

$$R_i=\frac{k_z}{k_y}\frac{d\langle u_{\parallel}\rangle}{dx}. \quad (4)$$

The fields ϕ , u_{\parallel} , and p are the Fourier amplitudes of potential, parallel ion flow, and ion pressure. These are normalized according to $\phi\equiv e\Phi/T_e$, $u_{\parallel}\equiv\tilde{v}_{\parallel i}/c_s$, and $p\equiv[\tilde{p}_i/\langle P_{i0}\rangle]\times(T_i/T_e)$, where $P_i=\langle P_{i0}\rangle+\tilde{p}_i$. Length scales are normalized to $\rho_s=(cT_e/eB)(m_i/T_e)^{1/2}$. In solving Eqs. (1)–(3), k_z is taken to be a constant. However reality of the fluctuation fields $\psi(\mathbf{x})$ leads to the parity constraints $\psi(-\mathbf{k})=\psi^*(\mathbf{k})$ and $\omega(-\mathbf{k})=-\omega^*(\mathbf{k})$, which include k_z . This means that the constant value of k_z changes sign when k_y changes sign.

This model is obviously simple, but it and similarly simple models have been frequently utilized particularly to understand nonlinear processes.^{9,22,23} The model does not include the flux-surface-averaged adiabatic response associated with zonal flows¹⁵ but is robustly saturated and regulated by the damped eigenmode that is conjugate to the unstable eigenmode. Equations (1)–(3) yield a conjugate pair of eigenmodes with the shear scaling of the slab ITG instability. The model shares a number of important physical behaviors with comprehensive gyrokinetic models.^{12,13} These include nonlinear cross phase angles, bursty transport fluxes, transport reductions from quasilinear values, highly broadened fixed-wavenumber frequency spectra, saturation time history with marked initial overshoot, limited broadening of the wavenumber spectrum beyond the range of linear instability, and the predilection for excitation of fluctuations at zonal wavenumbers, particularly $k_y=0$. The limited broadening of the wavenumber spectrum beyond the range of linear instability is an indication that there is significant fluctuation energy absorption within that range. This can only occur if damped eigenmodes are excited.

We examine the regime in which the mean parallel flow has a weak radial gradient. By weak gradient we mean the regime in which flow shear has a small effect on ITG instability, leaving $\nabla T_i\sim\hat{\eta}_i$ as the instability drive. From local linear stability analysis, this regime requires

$$\frac{1}{\hat{R}_i} = 1 + \frac{1}{R_i} \ll \frac{v_D k_y \hat{\eta}}{\omega}, \quad (5)$$

signifying moderate to large Richardson number. We treat the Richardson number as a parameter, implying that $d\langle u_{\parallel} \rangle/dx$ is taken as constant, the same way $d(\ln n_0)/dx$ is taken as constant in v_D . This is consistent with weak flow gradient. As a parameterization flow shear, the Richardson number labels flow gradient dependencies in fluxes.

A. Linear stability and conjugate structure

The eigenmode properties can be obtained from normal-mode solutions of the linearized equations. Linearizing Eqs. (1)–(3) and assuming a normal mode with frequency ω yield the dispersion relation

$$\omega^3(1+k^2) + k_y v_D \omega^2 (\hat{\eta} k^2 - 1) - \frac{k_z^2}{\hat{R}_i} \omega - k_y v_D k_z^2 \hat{\eta} = 0. \quad (6)$$

Cubic polynomials can be solved exactly. However, a simple approximation for the growth rate of the unstable mode is extremely useful for incorporating system symmetries into an order expansion that makes the eigenmode decomposition more transparent. The growth rate is approximated from a balance of the first and last terms of Eq. (6), valid when the second and third terms are small. This is formalized by introducing a small multiplier ϵ in the dispersion relation as follows: $\omega^3(1+k^2) + \epsilon k_y v_D \omega^2 (\hat{\eta} k^2 - 1) - \epsilon (k_z^2/\hat{R}_i) \omega - k_y v_D k_z^2 \hat{\eta} = 0$, and by expanding ω in powers of ϵ . Assuming $\omega = \omega^{(0)} + \epsilon \omega^{(1)} + \epsilon^2 \omega^{(2)} + \dots$, the two lowest order frequencies are given by

$$\omega_j^{(0)} = \left[\frac{k_y v_D k_z^2 \hat{\eta}}{1+k^2} \right]^{1/3} = S_j \left| \frac{k_y v_D k_z^2 \hat{\eta}}{1+k^2} \right|^{1/3}, \quad (7)$$

$$\omega_j^{(1)} = \frac{1}{S_j} \left(\frac{k_z^2}{3\hat{R}_i} \right) \left[\frac{1}{k_y v_D k_z^2 \hat{\eta} (1+k^2)^2} \right]^{1/3} - \frac{k_y v_D (\hat{\eta} k^2 - 1)}{3(1+k^2)}, \quad (8)$$

where $j=1-3$ labels the three branches and S_j , the cube root of 1, is

$$S_{1,3} = \left(-\frac{1}{2} \pm i \frac{\sqrt{3}}{2} \right), \quad (9)$$

$$S_2 = 1. \quad (10)$$

In Eq. (7) it is assumed that k_y and $k_z > 0$. For $k_y, k_z < 0$, S_j should be replaced by the cube root of -1 , i.e., $S_j \rightarrow -S_j^*$ for $\mathbf{k} \rightarrow -\mathbf{k}$.

There is a stable region ($\epsilon \ll 1$) with real-frequency roots for k_y very small. The roots are

$$\omega = 0, \quad (11)$$

$$\omega = \pm k_z / \hat{R}_i^{1/2} (1+k^2)^{1/2}, \quad (12)$$

obtained from the balance of the first and third terms in Eq. (6). The other region of stability occurs at high k_y , again with $\epsilon \ll 1$, where the first and second terms are dominant. This

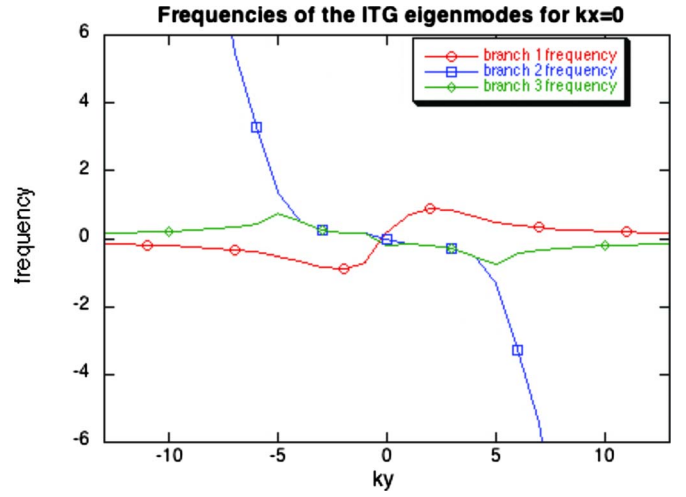


FIG. 1. (Color online) Real parts of three eigenfrequencies for a wavenumber range that includes the low- k_y and high- k_y stable ranges and the intermediate unstable range.

gives another set of real-frequency roots. Two roots have $\omega=0$, and the third has

$$\omega = -k_y v_D (\hat{\eta} k^2 - 1) / (1+k^2). \quad (13)$$

In the intermediate wavenumber range of instability, $\epsilon < 1$, and Eqs. (7) and (8) provide a reasonable approximation for the roots of the dispersion relation.

Because Eq. (6) is real, its solutions have complex-conjugate structure, i.e., if there is instability, the unstable and stable eigenmodes have growth rates that are equal and opposite and real frequencies that are equal. The third eigenmode is marginally stable. This applies to the frequencies of Eqs. (7) and (8), which satisfy $\omega_1 = \omega_3^*$, $\text{Im } \omega_2 = 0$. The frequencies of Eqs. (11)–(13) are outside the instability range and do not satisfy this symmetry property. If collisional processes leading to damping at high k are included in the dynamics, the coefficients of Eq. (6) are no longer real and the conjugate symmetry is broken. Figures 1 and 2 show the real

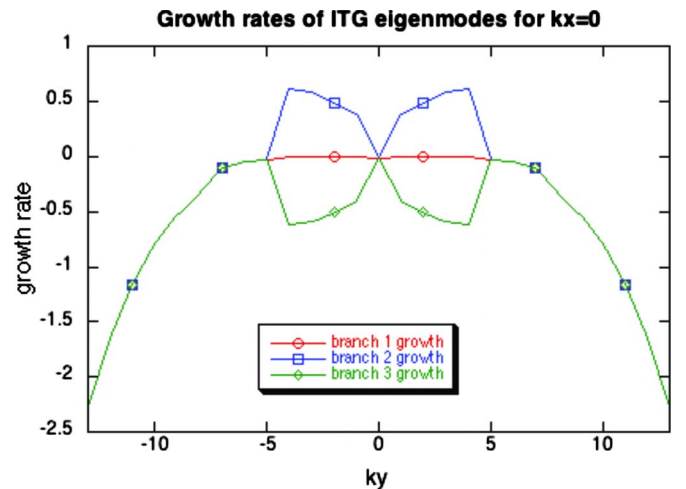


FIG. 2. (Color online) Growth rates from the imaginary parts of the eigenfrequencies for the same wavenumber range as in Fig. 1. Hyperviscous damping gives all branches a negative growth rate at large k_y , but the conjugate structure in the unstable region holds approximately.

and imaginary parts of the frequency for a case in which hyperviscous-type high- k damping has been added to the dispersion relation. The damping is configured in the three equations to preserve the eigenmode structure. The hyperviscosity coefficient in Figs. 1 and 2 is 0.8, giving a damping rate of 0.02 at the wavenumber of the maximum growth rate. This damping rate is 3% of the maximum growth rate of 0.65. With the hyperviscous damping, all three branches become damped at high k . However, in the region of instability the damping is sufficiently weak that the growth rate reflects the collisionless conjugate structure of Eqs. (7) and (8). Similarly, the real parts of the frequencies approximately follow the real parts of Eqs. (7)–(13). Consequently, the primary effect of hyperviscous-type damping is a modification of the collisionless dispersion to produce negative growth rates at high k . In the wavenumber range of instability, the mathematical structure of conjugate pairing remains in force.

The wavenumber range of the instability is described by the two conditions consistent with ϵ small, namely, $\omega^2(\hat{\eta}k^2 - 1) < k_z^2 \hat{\eta}$, corresponding to the first order- ϵ term of the dispersion relation being small, and $\omega/\hat{R}_i < k_y v_D \hat{\eta}$, corresponding to the second order- ϵ term being small. The second condition is the weak flow condition given in Eq. (5). If we substitute the lowest order frequency [Eq. (7)] for ω in these conditions, we can define two small quantities in terms of system parameters. We can then write the higher order terms of the expansion in terms of these quantities and set $\epsilon=1$ hereafter. From the first condition we define

$$\delta_p \equiv \frac{|\omega^{(0)}|^2(\hat{\eta}k^2 - 1)}{k_z^2 \hat{\eta}} = \frac{(\hat{\eta}k^2 - 1)}{\hat{\eta}} \left(\frac{k_y v_D \hat{\eta}}{k_z} \right)^{2/3} \frac{1}{(1+k^2)^{2/3}}, \quad (14)$$

and from the second condition we define

$$\alpha_p \equiv \frac{|\omega^{(0)}|}{k_y v_D \hat{\eta} \hat{R}_i} = \left(\frac{k_z}{k_y v_D \hat{\eta}} \right)^{2/3} \frac{1}{\hat{R}_i (1+k^2)^{1/3}}. \quad (15)$$

In terms of these parameters the frequency in the unstable range, through the two lowest orders, can be written

$$\omega_j = \left| \frac{k_y v_D k_z^2 \hat{\eta}}{1+k^2} \right|^{1/3} \left\{ S_j + \frac{1}{3} \left(\frac{\alpha_p}{S_j} - \delta_p \right) + O(\alpha_p^2) \right\}, \quad (16)$$

where the condition $\alpha_p \sim \delta_p < 1$ defines the validity range of the expansion. The flow shear dependence resides in α_p . In the regime of weak shear it has a stabilizing effect on the unstable eigenmode. Consistent with the conjugate structure, the damping rate of the stable eigenmode is reduced by flow shear.

B. Saturation and range of conjugate symmetry

In the conventional view of plasma turbulence, energy is transferred to a wavenumber region where the fastest growing mode becomes damped. The spectrum necessarily broadens into the region of negative growth rates, and saturation balances must include the physics of both the instability range and the nonoverlapping dissipation range. Equations (1)–(3) do not saturate in this way. Instead, the energy sinks that saturate the turbulence lie in the same wavenumber

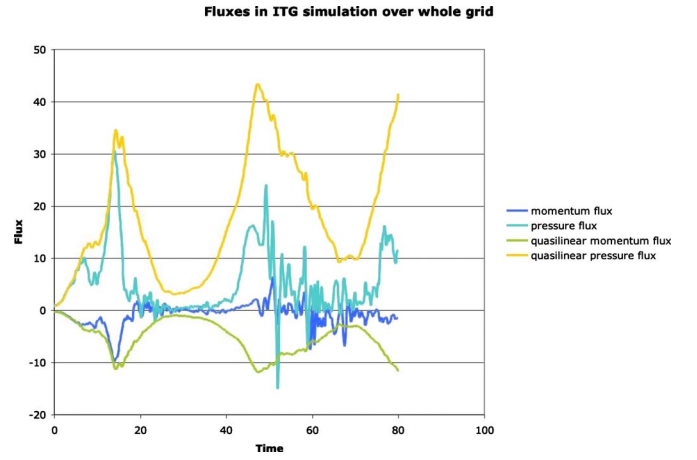


FIG. 3. (Color online) Momentum and heat fluxes and their quasilinear approximations. The fluxes are calculated by summing over all wavenumbers, including the high- k stable range dominated by hyperviscous damping.

range as the instability. To describe saturation, the energy transfer from unstable modes to separate damped eigenmodes in the same wavenumber range must be calculated. This transfer is present in solutions of comprehensive models but is hidden from view unless the solutions are projected onto an eigenmode basis.²⁰ In analytic theory damped eigenmodes must be treated explicitly, using the eigenmode decomposition or something comparable. This additional complicating factor in analysis is offset by a simplification. Because the instability saturates by transferring energy to damped eigenmode in the unstable wavenumber range, there is negligible spreading of the spectrum beyond the unstable range. This eliminates the need for careful resolution of modes outside the region of the instability, an aspect of gyrokinetic simulation for tokamak microinstability that has been recognized but not understood.²⁴

With energy confined to the unstable wavenumber range, Eqs. (7) and (8) are sufficient to generate the eigenmode decomposition and capture the saturation dynamics. We illustrate the extent to which transport is governed by modes within the wavenumber range of the instability by comparing fluxes computed solely from wavenumbers in the unstable range with fluxes that include wavenumbers over the entire spectrum. Figures 3 and 4 show the momentum flux $\chi_{||}$ and heat flux Q computed from a numerical solution of the model. The parameters, including wavenumber range, are the same as those used in Figs. 1 and 2 and include significant hyperviscous-type damping at high k . The wavenumbers range between 0.1 and 1.3 inverse gyroradii for both k_x and k_y . In Fig. 3 the wavenumber summation extends over the entire simulation grid, which goes well beyond the wavenumber range of the instability. Also plotted are the quasilinear approximations to the two fluxes. (These significantly overestimate the true fluxes because of the neglect the effect of the stable eigenmodes, as will be discussed in detail in Sec. IV.) Figure 4 shows the same fluxes computed by summing over the wavenumber range of the instability only. The differences between these two calculations are very slight. Despite strong hyperviscous-type damping at high k , almost

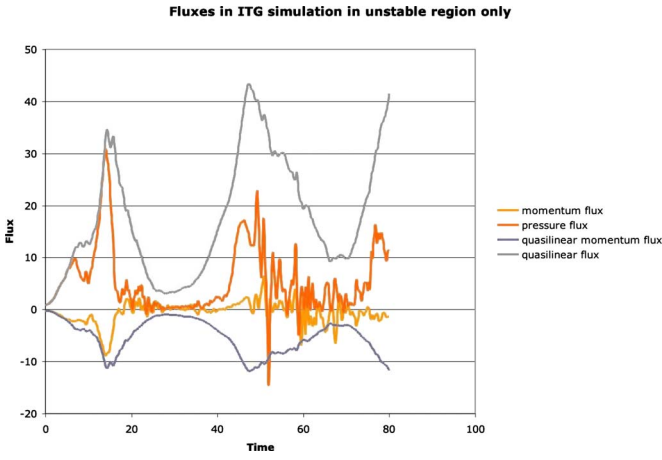


FIG. 4. (Color online) Momentum and heat fluxes and their quasilinear approximations as in Fig. 3. Here, however, the summations in the flux expressions are limited to the wavenumbers of the unstable range. This plot is nearly the same as Fig. 3, with slight differences. The close similarity with Fig. 3 indicates that the fluctuation energy is mostly confined to the unstable region and hyperviscous damping has little effect.

no energy gets there, and fluctuations outside the unstable wavenumber range play a negligible role in the dynamics of transport.

Given this property of saturation, the expansion of the dispersion in Eq. (16) is all that is needed to describe dissipation and damping in the turbulent system and to compute eigenvectors for the eigenmode decomposition. Moreover, the symmetries encapsulated in the three roots of the unstable region are those that characterize the turbulence and its nonlinear dynamics.

III. MOMENTUM AND HEAT FLUXES IN EIGENMODE DECOMPOSITION

Figure 2 in Ref. 12 shows the evolution of the squared amplitudes of the three eigenmodes whose frequencies are given in Eqs. (7) and (8). All three reach comparable levels in saturation. Quasilinear flux expressions depend only on the amplitude of the unstable mode. Because the other two eigenmodes have a comparable level in saturation, it is important to account for their contribution to transport fluxes. In this section we derive heat and momentum flux expressions that include the contribution of all three eigenmodes. These expressions have a symmetric structure associated

with the conjugate symmetry of the instability and the damped eigenmode. The symmetry links the two fluxes derivable from Eqs. (1)–(3) in a way that is not evident when they are written in the usual form as correlations of primitive fields.

The two transport fluxes described within the model are fluxes of heat and parallel flow, associated with the $E \times B$ advection of pressure and parallel flow fluctuations. These are given by $\mathbf{Q} = -\langle \nabla \phi \times \hat{\mathbf{z}} \cdot \mathbf{p} \rangle$ and $\chi_{\parallel} = -\langle \nabla \phi \times \hat{\mathbf{z}} \cdot u_{\parallel} \rangle$. In the Fourier representation the radial components are

$$\mathbf{Q} \cdot \hat{\mathbf{r}} = - \sum_k k_y \text{Im} \langle \phi_{-k} p_k \rangle, \quad (17)$$

$$\chi_{\parallel} \cdot \hat{\mathbf{r}} = - \sum_k k_y \text{Im} \langle \phi_{-k} u_{\parallel k} \rangle. \quad (18)$$

We will refer to χ_{\parallel} as the momentum flux.

The fields p , u_{\parallel} , and ϕ can be projected onto the three eigenvectors corresponding to the eigenfrequencies of Eqs. (7) and (8). The decomposition is

$$\begin{pmatrix} p \\ u_{\parallel} \\ \phi \end{pmatrix} = \begin{pmatrix} b_1 & b_2 & b_3 \\ a_1 & a_2 & a_3 \\ 1 & 1 & 1 \end{pmatrix} \begin{pmatrix} \beta_1 \\ \beta_2 \\ \beta_3 \end{pmatrix} \equiv \mathbf{M} \begin{pmatrix} \beta_1 \\ \beta_2 \\ \beta_3 \end{pmatrix}, \quad (19)$$

where $(b_j, a_j, 1)$ is the eigenvector corresponding to the frequency ω_j and β_j is the coefficient of the j th eigenvector in the decomposition. In the Fourier representation, p , u_{\parallel} , and ϕ are functions of k , making b_j , a_j , and β_j functions of k . The eigenvectors are nonorthogonal but form a complete set. The coefficients β_j are arbitrary in the linear eigenvalue problem. In the linear initial value problem they are set by the initial conditions $\beta_j(t=0) = \beta_{j0}$ and evolve as normal modes $\beta_{jk}(t) = \beta_{j0k} \exp[i\omega_j(k)t]$. Nonlinearly, exponentially growing eigenmodes β_{jk} are saturated by energy transfer associated with Fourier-mode coupling between eigenmodes $\beta_{lk'}$ and $\beta_{mk''}$, where $k = k' + k''$. The mode coupling is specified by the evolution equations, Eqs. (1)–(3), once they have been transformed using Eq. (19) to the representation of β_j . The nonlinear equations for β_j are given later in this paper in Eq. (35). Figure 2 in Ref. 12 shows the evolution of $|\beta_j|^2$. In this paper we derive expressions for the eigenvector components b_j and a_j and use them in the fluxes.

When Eq. (19) is substituted into Eqs. (17) and (18), the fluxes are given by

$$\begin{aligned} \mathbf{Q} \cdot \hat{\mathbf{r}} = & - \sum_k k_y \{ \text{Im} b_1(k) |\beta_1|^2 + \text{Im} b_2(k) |\beta_2|^2 + \text{Im} b_3(k) |\beta_3|^2 + [\text{Im} b_1(k) + \text{Im} b_2(k)] \text{Re} \langle \beta_1 \beta_2^* \rangle \\ & + [\text{Im} b_2(k) + \text{Im} b_3(k)] \text{Re} \langle \beta_2 \beta_3^* \rangle + [\text{Im} b_1(k) + \text{Im} b_3(k)] \text{Re} \langle \beta_1 \beta_3^* \rangle + [\text{Re} b_1(k) - \text{Re} b_2(k)] \text{Im} \langle \beta_1 \beta_2^* \rangle \\ & + [\text{Re} b_2(k) - \text{Re} b_3(k)] \text{Im} \langle \beta_2 \beta_3^* \rangle + [\text{Re} b_1(k) - \text{Re} b_3(k)] \text{Im} \langle \beta_1 \beta_3^* \rangle \} \end{aligned} \quad (20)$$

and

$$\begin{aligned}
\chi_{\parallel} \cdot \hat{r} = & - \sum_k k_y \{ \text{Im } a_1(k) |\beta_1|^2 + \text{Im } a_2(k) |\beta_2|^2 + \text{Im } a_3(k) |\beta_3|^2 + [\text{Im } a_1(k) + \text{Im } a_2(k)] \text{Re} \langle \beta_1 \beta_2^* \rangle \\
& + [\text{Im } a_2(k) + \text{Im } a_3(k)] \text{Re} \langle \beta_2 \beta_3^* \rangle + [\text{Im } a_1(k) + \text{Im } a_3(k)] \text{Re} \langle \beta_1 \beta_3^* \rangle + [\text{Re } a_1(k) - \text{Re } a_2(k)] \text{Im} \langle \beta_1 \beta_2^* \rangle \\
& + [\text{Re } a_2(k) - \text{Re } a_3(k)] \text{Im} \langle \beta_2 \beta_3^* \rangle + [\text{Re } a_1(k) - \text{Re } a_3(k)] \text{Im} \langle \beta_1 \beta_3^* \rangle \}. \quad (21)
\end{aligned}$$

In writing these expressions we have used $\phi_{-k} = \phi_k^* = \beta_1^* + \beta_2^* + \beta_3^*$. The first term of each of these expressions represents the quasilinear flux. The remaining terms are contributions from the stable eigenmodes. Because the eigenvectors are not orthogonal, the fluxes depend on both the positive-definite squared amplitudes $|\beta_j|^2$ and the complex-valued cross correlations $\langle \beta_j \beta_k^* \rangle$.

We now derive the eigenvector components b_j and a_j . This exercise is made much simpler by the restriction of dynamical activity to the wavenumber range of the instability, as discussed in the previous section. The eigenvectors describe the field ratios p_j/ϕ_j and $u_{\parallel j}/\phi_j$ of the linearized evolution equations when $\omega = \omega_j$. With the eigenvectors normalized so that $\phi_j = 1$,

$$b_j = \frac{p_j}{\phi_j} = \frac{k_y v_D \hat{\eta}}{\omega_j}, \quad (22)$$

$$a_j = \frac{u_{\parallel j}}{\phi_j} = \frac{k_z}{\omega_j} + \frac{k_z k_y v_D \hat{\eta}}{\omega_j^2}. \quad (23)$$

Substituting Eq. (16) into Eqs. (22) and (23) and expanding for $\alpha_p \sim \delta_p \ll 1$ yield

$$b_j = \frac{1}{\alpha_p \hat{R}_i} \left[S_j^* - \frac{1}{3} \alpha_p + \frac{1}{3} \delta_p S_j + \text{O}(\alpha_p^2) \right], \quad (24)$$

$$a_j = \left[\frac{(1+k^2)}{\alpha_p \hat{R}_i} \right]^{1/2} \left[S_j + \frac{1}{3} \alpha_p S_j^* + \frac{2}{3} \delta_p + \text{O}(\alpha_p^2) \right]. \quad (25)$$

The conjugate structure of the eigenfrequencies imposes conjugate structure on the eigenvectors. This is expressed in the relations

$$a_1 = a_3^*, \quad (26)$$

$$b_1 = b_3^*, \quad (27)$$

$$\text{Im } a_2 = \text{Im } b_2 = 0. \quad (28)$$

As a result of these identities the coefficients of $\text{Re} \langle \beta_1 \beta_3^* \rangle$ and $\text{Im} \langle \beta_1 \beta_3^* \rangle$ are zero, making these correlations drop out of both fluxes. The coefficient of $\text{Re} \langle \beta_1 \beta_2^* \rangle$ is the same as that of $|\beta_1|^2$, which is equal and opposite to the coefficients of $|\beta_3|^2$ and $\text{Re} \langle \beta_2^* \beta_3 \rangle$. With these simplifications the fluxes can be written as

$$\begin{aligned}
\mathbf{Q} \cdot \hat{r} = & \sum_k k_y \left[\frac{1}{\alpha_p \hat{R}_i} \right] \left\{ \frac{\sqrt{3}}{2} \left(1 - \frac{1}{3} \delta_p \right) \right. \\
& \times (|\beta_1|^2 - |\beta_3|^2 + \text{Re} \langle \beta_1 \beta_2^* \rangle - \text{Re} \langle \beta_2 \beta_3^* \rangle) \\
& \left. - \left(\frac{3}{2} + \frac{2}{3} \delta_p \right) (\text{Im} \langle \beta_2 \beta_3^* \rangle - \text{Im} \langle \beta_1 \beta_2^* \rangle) \right\}, \quad (29)
\end{aligned}$$

$$\begin{aligned}
\chi_{\parallel} \cdot \hat{r} = & - \sum_k k_y \left[\frac{1+k^2}{\alpha_p \hat{R}_i} \right]^{1/2} \left\{ \frac{\sqrt{3}}{2} \left(1 - \frac{1}{3} \alpha_p \right) \right. \\
& \times (|\beta_1|^2 - |\beta_3|^2 + \text{Re} \langle \beta_1 \beta_2^* \rangle - \text{Re} \langle \beta_2 \beta_3^* \rangle) \\
& \left. + \left(\frac{3}{2} + \frac{2}{3} \delta_p + \frac{1}{2} \alpha_p \right) (\text{Im} \langle \beta_2 \beta_3^* \rangle - \text{Im} \langle \beta_1 \beta_2^* \rangle) \right\}. \quad (30)
\end{aligned}$$

The quasilinear fluxes are recovered when the correlations $\langle \phi_{-k} p_k \rangle$ and $\langle \phi_{-k} u_{\parallel k} \rangle$ depend only on the unstable eigenmode. This corresponds to setting $\beta_2 = \beta_3 = 0$ in Eqs. (29) and (30), leaving only the terms proportional to $|\beta_1|^2$. Note that with $\beta_2 = \beta_3 = 0$, $\phi = \beta_1$, making this the usual form of the quasilinear flux. When $\beta_2, \beta_3 \neq 0$, we continue to call the terms proportional to $|\beta_1|^2$ quasilinear fluxes, although these are different from what would be computed from $\sum k_y \text{Im } b_1(k) |\phi_k|^2$ and $\sum k_y \text{Im } a_1(k) |\phi_k|^2$ because $\beta_1 \neq \phi$. Note that under the parity constraints $\psi(-\mathbf{k}) = \psi^*(\mathbf{k})$ and $\omega(-\mathbf{k}) = -\omega^*(\mathbf{k})$, the summands of $\mathbf{Q} \cdot \hat{r}$ and $\chi_{\parallel} \cdot \hat{r}$ have even parity in $\mathbf{k} = (k_x, k_y, k_z)$. This is most easily verified from the quasilinear expressions involving $\text{Im } b_1(k)$ and $\text{Im } a_1(k)$ just given but is true in general.

Looking at Eqs. (29) and (30), we observe that in relation to the quasilinear fluxes, the true fluxes are much more complex. Nevertheless, we can learn a great deal about the transport from the form of Eqs. (29) and (30), even without a solution for the correlations $|\beta_1|^2$, $|\beta_2|^2$, $\langle \beta_1 \beta_2^* \rangle$, and $\langle \beta_2 \beta_3^* \rangle$. It is particularly revealing to consider the relative forms of the two fluxes in conjunction with the thermodynamic constraint that precludes transport up the gradient that drives instability. The thermodynamic constraint applies only to the flux that is diagonal in the driving gradient, not the other. However, the forms have a high degree of isomorphism, through which the thermodynamic constraint can be used to make inferences about the behavior of the other flux.

First, however, we consider which correlations are missing from Eqs. (29) and (30) and what that represents. The positive-definite autocorrelation of the marginal eigenmode $|\beta_2|^2$ does not appear in either flux because, with no damping or growth, its contribution to the transport correlations

$\langle \phi_{-k} p_k \rangle$ and $\langle \phi_{-k} u_{\parallel k} \rangle$ makes ϕ_{-k} in phase with p_k and $u_{\parallel k}$. In-phase correlations give no transport. Mathematically this is imposed by $\text{Im } a_2 = \text{Im } b_2 = 0$. The positive-definite auto-correlation of the damped eigenmode $|\beta_3|^2$ is such as to reduce the contribution to the fluxes made by the unstable eigenmode $|\beta_1|^2$, i.e., to reduce the quasilinear flux. This is again a simple consequence of phases. When the unstable eigenmode gives outward transport, the stable eigenmode, with its 180° phase difference relative to the unstable eigenmode, gives inward transport.¹¹ The damped eigenmode β_3 is excited by energy transfer from the unstable eigenmode β_1 . Yet the correlation $\langle \beta_1 \beta_3^* \rangle$ does not appear in either flux because conjugate symmetry makes the coefficients of $\text{Re}\langle \beta_1 \beta_3^* \rangle$ and $\text{Im}\langle \beta_1 \beta_3^* \rangle$ zero. This implies that β_2 is an important mediator in energy transfer, at least as far as fluxes are concerned. The correlations $\langle \beta_1 \beta_2^* \rangle$ and $\langle \beta_2 \beta_3^* \rangle$ do contribute to the fluxes. The way these correlations enter the two fluxes is also structured by conjugate symmetry.

The isomorphism of structure in the two fluxes alluded to previously applies to the way the correlations enter the two fluxes. All eigenmode correlations that contribute to transport do so in the same combinations $\{|\beta_1|^2 - |\beta_3|^2 + \text{Re}\langle \beta_1 \beta_2^* \rangle - \text{Re}\langle \beta_2 \beta_3^* \rangle\}$ and $\{\text{Im}\langle \beta_2 \beta_3^* \rangle - \text{Im}\langle \beta_1 \beta_2^* \rangle\}$. The coefficients of these combinations are different in the two fluxes. However, apart from the overall factors $1/(\alpha_p \hat{R}_i)$ and $-[(1+k^2)/\alpha_p \hat{R}_i]^{1/2}$ in the heat and momentum fluxes, respectively, the residual coefficients inside the $\{ \}$ brackets differ only by factors of $(\sqrt{3}/2)/(3/2) = 1/\sqrt{3}$ and/or the higher order terms of the expansion in $\alpha_p(\delta_p)$. The isomorphism of the eigenmode correlations is significant to the degree to which the residual coefficients are nearly equal. The residual coefficients of $\{|\beta_1|^2 - |\beta_3|^2 + \text{Re}\langle \beta_1 \beta_2^* \rangle - \text{Re}\langle \beta_2 \beta_3^* \rangle\}$ in the heat and momentum fluxes are equal in lowest order, and hence have the same sign. Given the opposite signs of the overall factors, the heat flux associated with $\{|\beta_1|^2 - |\beta_3|^2 + \text{Re}\langle \beta_1 \beta_2^* \rangle - \text{Re}\langle \beta_2 \beta_3^* \rangle\}$ is outward, and the momentum flux is inward. Significantly, the residual coefficients of $\{|\beta_1|^2 - |\beta_3|^2 + \text{Re}\langle \beta_1 \beta_2^* \rangle - \text{Re}\langle \beta_2 \beta_3^* \rangle\}$ and $\{\text{Im}\langle \beta_2 \beta_3^* \rangle - \text{Im}\langle \beta_1 \beta_2^* \rangle\}$ have the same sign in the momentum flux and opposite signs in the heat flux. This makes the isomorphism imperfect and prevents the thermodynamic constraint from applying to both fluxes unless $\{\text{Im}\langle \beta_2 \beta_3^* \rangle - \text{Im}\langle \beta_1 \beta_2^* \rangle\} = 0$.

The thermodynamic constraint applies to the heat flux because it is diagonal in the temperature gradient, which drives the instability. (The coefficients in the heat flux have no dependence on the flow gradient through the two lowest orders because the flow gradient cancels out of $\alpha_p \hat{R}_i$.) The coefficient of $|\beta_1|^2$ is positive, so the quasilinear heat flux is outward, satisfying the thermodynamic constraint. The diagonal part of the momentum flux is proportional to flow gradient, which resides in α_p and is smaller than the off-diagonal part proportional to temperature gradient. Hence the flux can be inward, which it is for quasilinear theory. Let us assume for the moment that the cross correlation terms nearly cancel one another (i.e., $\text{Re}\langle \beta_1 \beta_2^* \rangle \approx \text{Re}\langle \beta_2 \beta_3^* \rangle$ and $\text{Im}\langle \beta_2 \beta_3^* \rangle \approx \text{Im}\langle \beta_1 \beta_2^* \rangle$). In the next section we will show that this is often the case. In this situation we see that the damped

eigenmode reduces the quasilinear heat flux. However, it cannot reduce the heat flux to the point where $|\beta_1|^2 - |\beta_3|^2 < 0$ because this would make the flux inward and violate thermodynamics. Because the momentum flux depends on the same combination $|\beta_1|^2 - |\beta_3|^2$, it too is reduced but not so much to change its sign and make it outward. If we now allow that $\text{Re}\langle \beta_1 \beta_2^* \rangle - \text{Re}\langle \beta_2 \beta_3^* \rangle \neq 0$ (but $\text{Im}\langle \beta_2 \beta_3^* \rangle \approx \text{Im}\langle \beta_1 \beta_2^* \rangle$), the situation is unchanged. Whatever $-|\beta_3|^2 + \text{Re}\langle \beta_1 \beta_2^* \rangle - \text{Re}\langle \beta_2 \beta_3^* \rangle$ does to $|\beta_1|^2$ in the heat flux, it does the same in the momentum flux. Since the heat flux cannot become inward, the momentum flux cannot become outward.

Consider now the terms proportional to $\text{Im}\langle \beta_2 \beta_3^* \rangle - \text{Im}\langle \beta_1 \beta_2^* \rangle$. These terms have opposite signs in the heat and momentum fluxes relative to the terms proportional to $\{|\beta_1|^2 - |\beta_3|^2 + \text{Re}\langle \beta_1 \beta_2^* \rangle - \text{Re}\langle \beta_2 \beta_3^* \rangle\}$. Here the thermodynamic constraint no longer keeps the momentum flux inward. To see how the momentum flux can become outward, assume that $\text{Im}\langle \beta_2 \beta_3^* \rangle - \text{Im}\langle \beta_1 \beta_2^* \rangle$ is negative. In the heat flux this term has a negative coefficient. Hence it contributes to outward transport, and the thermodynamic constraint cannot limit its magnitude. In the momentum flux this term has a positive coefficient, so it contributes to outward momentum transport. With its magnitude unconstrained it can overwhelm the other terms and reverse the sign of the flux relative to the quasilinear value.

IV. EIGENMODE CORRELATIONS

We return to Fig. 3 and the prominent feature that the magnitude of the quasilinear fluxes is greater than the true fluxes. The fluxes are bursty, and this difference is greatest away from the peaks. The burstiness, which occurs despite fixed equilibrium gradients, was analyzed statistically in Ref. 12 and shown to have intermittent features associated with long range temporal correlations. In terms of the discussion of the previous section, an aspect of the burstiness is a dynamical transition from situations in which the unstable eigenmode dominates the stable eigenmodes to situations with greater parity. This toggling between situations in which damped eigenmodes are subdominant and dominant is also a feature observed in gyrokinetic simulations.²⁰ The quasilinear fluxes for heat and momentum are outward and inward, respectively, as discussed in the previous section. For the most part the true fluxes retain the same sign. However, there are occasions when the momentum flux reverses sign and becomes time average outward over time windows that include multiple correlation times.

For more detailed analysis of this behavior, we need to know the eigenmode correlations on which the fluxes depend. Because stable eigenmodes are excited by nonlinear energy transfer, their levels and cross correlations are a matter of saturation energetics. Therefore we first consider the eigenmode correlations of the energy. Like the flux the energy can be expanded using the eigenmode decomposition and represented in terms of quadratic correlations. The function given by

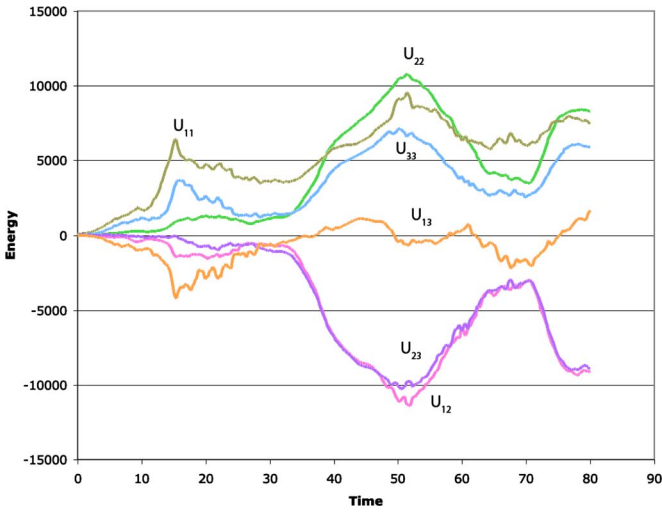


FIG. 5. (Color online) Energy components in the eigenmode decomposition. The energy related to the cross correlation between the unstable and damped eigenmodes is the smallest and fluctuates around zero.

$$U = \sum_k [(1+k^2)|\phi|^2 + |u_{\parallel}|^2 + |p|^2] \quad (31)$$

is quadratic in the three fluctuating fields, an invariant of the nonlinearities, and consequently a suitable definition of energy. Using the decomposition of Eq. (19), the energy can be written as

$$U = U_{11} + U_{22} + U_{33} + U_{12} + U_{13} + U_{23}, \quad (32)$$

where

$$U_{jj} = \sum_k [(1+k^2) + |a_j|^2 + |b_j|^2] |\beta_j|^2 \quad (33)$$

are the positive-definite energies associated with each eigenmode and

$$U_{jk} = \sum_k \{ [(1+k^2) + 2 \operatorname{Re}(a_j a_k^*) + 2 \operatorname{Re}(b_j b_k^*)] \operatorname{Re}\langle \beta_j \beta_k^* \rangle - [2 \operatorname{Im}(a_j a_k^*) + 2 \operatorname{Im}(b_j b_k^*)] \operatorname{Im}\langle \beta_j \beta_k^* \rangle \} \quad (34)$$

are the components related to each cross correlation. Unlike the flux, the coefficients of $\operatorname{Re}\langle \beta_1 \beta_3^* \rangle$ and $\operatorname{Im}\langle \beta_1 \beta_3^* \rangle$ are not zero because of conjugate symmetry. The correlation between the unstable and stable modes therefore contributes to the energy.

The quantities U_{jj} and U_{jk} are plotted in Fig. 5 for the same saturated state depicted in Figs. 3 and 4. We note that the three eigenmode energies U_{jj} are all comparable in saturation. The most striking feature in Fig. 5 is the small magnitude of U_{13} relative to U_{12} and U_{23} after 40 time units and the near equality of U_{12} and U_{23} for most of the time. These two features indicate that the dominant channel of energy transfer is from the unstable to the damped eigenmode through the intermediary of the marginal mode. The small value of U_{13} indicates a weak $\langle \beta_1 \beta_3^* \rangle$ correlation and relatively little direct transfer from unstable to damped mode. The near equality of U_{12} and U_{23} suggests that conjugate symmetry creates a near mirror image situation between the correlation of growing and marginal mode and that of mar-

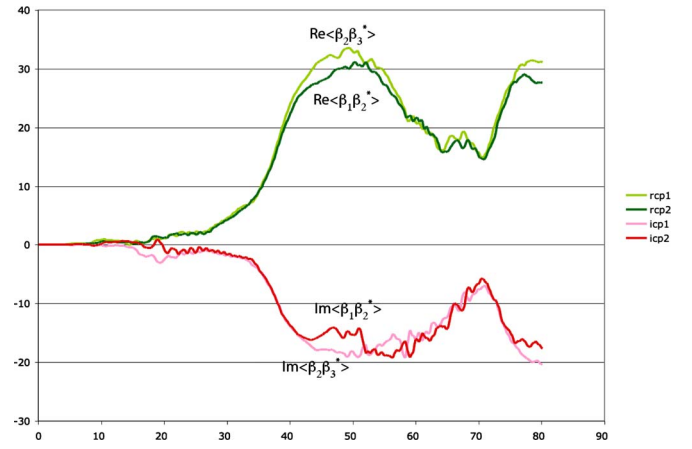


FIG. 6. (Color online) Real and imaginary parts of the cross correlations between unstable and marginally stable and marginally stable and damped-eigenmode branches. The real parts of the two correlations are nearly equal some of the time, as are the imaginary parts. During other times values are similar but not equal.

ginal mode and damped mode. The energies U_{11} and U_{33} are not equal because one corresponds to a source and one to a sink. Nevertheless, U_{33} is sufficiently large to indicate that dissipation of damped-eigenmode energy is the primary saturation mechanism, as opposed to the usual cascade to high k . We note that $U_{22} > U_{11}$ on occasion, again indicating its important role as an intermediary in the energy transfer.

The near equality of U_{12} and U_{23} raises the question as to whether there might be some cancellation of the cross correlation terms in the fluxes. Figure 6 shows the cross products $\operatorname{Re}\langle \beta_1 \beta_2^* \rangle$, $\operatorname{Re}\langle \beta_2 \beta_3^* \rangle$, $\operatorname{Im}\langle \beta_1 \beta_2^* \rangle$, and $\operatorname{Im}\langle \beta_2 \beta_3^* \rangle$. Indeed the two real parts are nearly equal most of the time, as are the two imaginary parts. Consequently the cross correlations nearly cancel out of the fluxes in Eqs. (29) and (30) so that they are governed primarily by the autocorrelation factor $|\beta_1|^2 - |\beta_2|^2$. When this is true the role of stable eigenmodes is simple: they reduce the quasilinear fluxes but do not change the direction of transport. However, there are periods when $\operatorname{Re}\langle \beta_1 \beta_2^* \rangle \neq \operatorname{Re}\langle \beta_2 \beta_3^* \rangle$ and $\operatorname{Im}\langle \beta_1 \beta_2^* \rangle \neq \operatorname{Im}\langle \beta_2 \beta_3^* \rangle$. In Fig. 6 one such period is between 40 and 60 time units. If we examine the fluxes in Fig. 3 (which are for the same simulation), we observe that during this time, the momentum flux changes sign and becomes outward on time average, although it is small. The heat flux also has spikes in which it becomes inward briefly, but the time average remains outward. This is precisely the situation discussed in the previous section where the isomorphism of the heat and momentum fluxes is broken by nonzero cross correlations. We note that the simulation results are consistent with the implications drawn from the analysis of the thermodynamic constraint in conjunction with the near isomorphism of the fluxes.

We examine the evolution equations for $\langle \beta_1 \beta_2^* \rangle$ and $\langle \beta_2 \beta_3^* \rangle$ to determine if general features evident in Fig. 6 can be extracted without solving for higher order correlations, much as we did with Eqs. (29) and (30) for the fluxes. We do not have a principle such as the thermodynamic constraint that works singly on one of these expressions. However, we can compare the two expressions and investigate the effect of

conjugate symmetry. To proceed we transform the original dynamical equations to the eigenmode decomposition, yielding

$$\begin{pmatrix} \dot{\beta}_1 \\ \dot{\beta}_2 \\ \dot{\beta}_3 \end{pmatrix} = \begin{pmatrix} i\omega_1 & 0 & 0 \\ 0 & i\omega_2 & 0 \\ 0 & 0 & i\omega_3 \end{pmatrix} \begin{pmatrix} \beta_1 \\ \beta_2 \\ \beta_3 \end{pmatrix} = \mathbf{M}^{-1} \begin{pmatrix} N_p \\ N_{u_\parallel} \\ N_\phi \end{pmatrix}. \quad (35)$$

We multiply the equation for $\dot{\beta}_1$ by β_2^* and add it to the equation for $\dot{\beta}_2^*$ multiplied by β_1 to obtain the equation for $\partial\langle\beta_1\beta_2^*\rangle/\partial t$. We evaluate \mathbf{M}^{-1} , and obtain

$$\begin{aligned} & \frac{\partial}{\partial t} \langle \beta_1 \beta_2^* \rangle - i\omega_1 \langle \beta_1 \beta_2^* \rangle + i\omega_2^* \langle \beta_1 \beta_2^* \rangle \\ &= \frac{1}{\text{Det } \mathbf{M}} [(a_2 - a_3) \langle N_p \beta_2^* \rangle + (b_3 - b_2) \langle N_{u_\parallel} \beta_2^* \rangle \\ &+ (b_2 a_3 - b_3 a_2) \langle N_\phi \beta_2^* \rangle] + \frac{1}{(\text{Det } \mathbf{M})^*} \\ &\times [(a_3^* - a_1^*) \langle N_p \beta_1 \rangle + (b_1^* - b_3^*) \langle N_{u_\parallel} \beta_1 \rangle \\ &+ (b_3^* a_1^* - b_1^* a_3^*) \langle N_\phi \beta_1 \rangle], \end{aligned} \quad (36)$$

where $\text{Det } \mathbf{M} = b_1 a_2 + b_2 a_3 + b_3 a_1 - b_3 a_2 - b_2 a_1 - b_1 a_3$. Similarly,

$$\begin{aligned} & \frac{\partial}{\partial t} \langle \beta_2 \beta_3^* \rangle - i\omega_2 \langle \beta_2 \beta_3^* \rangle + i\omega_3^* \langle \beta_2 \beta_3^* \rangle \\ &= \frac{1}{\text{Det } \mathbf{M}} [(a_3 - a_1) \langle N_p \beta_3^* \rangle + (b_1 - b_3) \langle N_{u_\parallel} \beta_3^* \rangle \\ &+ (b_3 a_1 - b_1 a_3) \langle N_\phi \beta_3^* \rangle] + \frac{1}{(\text{Det } \mathbf{M})^*} \\ &\times [(a_1^* - a_2^*) \langle N_p \beta_2 \rangle + (b_2^* - b_1^*) \langle N_{u_\parallel} \beta_2 \rangle \\ &+ (b_1^* a_2^* - b_2^* a_1^*) \langle N_\phi \beta_2 \rangle]. \end{aligned} \quad (37)$$

Using Eq. (19) the nonlinearities can be expressed as quadratic correlations of eigenmode amplitudes β_j at wavenumbers k' and k'' . For example, $N_\phi = -(1+k^2)^{-1} \sum_{k'} (\mathbf{k}' \times \mathbf{z} \cdot \mathbf{k}) \times [\beta_1(k') + \beta_2(k') + \beta_3(k')] [\beta_1(k-k') + \beta_2(k-k') + \beta_3(k-k')]$. This makes the factors such as $\langle N_p \beta_2^* \rangle$ a series of triplet correlations.

We impose conjugate symmetry by eliminating a_3 and b_3 using Eqs. (26) and (27). Equations (36) and (37) then can be written as

$$\begin{aligned} & \frac{\partial}{\partial t} \langle \beta_1 \beta_2^* \rangle - i(\omega_1 - \omega_2^*) \langle \beta_1 \beta_2^* \rangle \\ &= \frac{1}{\text{Det } \mathbf{M}} \{ [(a_2^* - a_1^*) \langle N_p \beta_2^* \rangle + (b_1^* - b_2^*) \langle N_{u_\parallel} \beta_2^* \rangle \\ &+ (b_2^* a_1^* - b_1^* a_2^*) \langle N_\phi \beta_2^* \rangle] - 2i [\text{Im } a_1 \langle N_p \beta_1 \rangle \\ &- \text{Im } b_1 \langle N_{u_\parallel} \beta_1 \rangle + \text{Im}(b_1 a_1^*) \langle N_\phi \beta_1 \rangle] \} \end{aligned} \quad (38)$$

and

$$\begin{aligned} & \frac{\partial}{\partial t} \langle \beta_2 \beta_3^* \rangle + i(\omega_1 - \omega_2^*) \langle \beta_2 \beta_3^* \rangle \\ &= \frac{1}{\text{Det } \mathbf{M}} \{ [(a_2^* - a_1^*) \langle N_p \beta_2^* \rangle + (b_1^* - b_2^*) \langle N_{u_\parallel} \beta_2^* \rangle \\ &+ (b_2^* a_1^* - b_1^* a_2^*) \langle N_\phi \beta_2^* \rangle] - 2i [\text{Im } a_1 \langle N_p \beta_3^* \rangle \\ &- \text{Im } b_1 \langle N_{u_\parallel} \beta_3^* \rangle + \text{Im}(b_1 a_1^*) \langle N_\phi \beta_3^* \rangle] \}, \end{aligned} \quad (39)$$

where $(\text{Det } \mathbf{M})^* = -\text{Det } \mathbf{M}$, a property that follows from conjugate symmetry, has been imposed. Comparing Eqs. (38) and (39) we note that the nonlinear forces driving these two correlations are almost identical but also have crucial differences. The forces proportional to correlations of β_2 with the nonlinearities are identical up to a complex-conjugate operation on triplet correlations. The remaining forces have the same complex-conjugate structure, with β_1 appearing in correlations with the nonlinearities in Eq. (38) and β_3 appearing in the correlations with nonlinearities in Eq. (39). These forces are sufficiently close to being identical that it is not surprising that $\langle \beta_1 \beta_2^* \rangle$ and $\langle \beta_2 \beta_3^* \rangle$ could be nearly the same part of the time. On the other hand the differences in the forces leave room for the two correlations to become different at times. It is not easy to identify from Eqs. (38) and (39) what might trigger shifts between the two types of behavior. Further inferences of behavior evidently will require detailed information on the triplet correlations.

V. DISCUSSION AND CONCLUSIONS

We have considered three issues relating to the role of damped eigenmodes on momentum transport. First, we have shown that the damped eigenmode that saturates ITG turbulence in a reduced fluid model decreases the inward momentum flux. Second, we have shown that damped eigenmodes create a significant structural link between the heat and momentum fluxes, even though the former is diagonal and subject to a thermodynamic constraint and the latter is not. Third, we have traced how the conjugate-pair relationship between the unstable and damped branches affects damped-eigenmode excitation, saturation, and transport through the wavenumber dependencies of growth rates, frequencies, and eigenvectors.

In the eigenmode decomposition the momentum flux can be written as the sum of a quasilinear component, which is proportional to the autocorrelation of the unstable eigenmode amplitude, and a nonlinear component. The latter is comprised of a negative-definite term proportional to the autocorrelation of the damped-eigenmode amplitude and eigenmode cross correlation terms of indefinite sign. (In systems with more than one damped eigenmode, there is one negative-definite autocorrelation for each damped eigenmode in the system.) The flux evolves in a bursty fashion, with the cross correlation terms often canceling to a significant degree. When this is true the momentum flux is governed by the simple competing effects of unstable and stable eigenmodes, which drive transport in opposite directions. The cancellation of the cross correlation terms is related to the high degree of symmetry between the unstable and stable eigenmodes,

which in the reduced ITG model form a complex-conjugate pair. While the excitation of damped eigenmodes seems to be a very robust and common phenomenon across many models, the effect on fluxes is varied and likely depends on the kind of symmetry or lack of symmetry between unstable and stable eigenmodes. The reduction seen in the reduced ITG model is weaker in some gyrokinetic simulations and nearly absent in others.

The momentum and heat fluxes are nearly isomorphic in the eigenmode decomposition, as reflected in Eqs. (29) and (30). The parallel structures differ only in coefficients of eigenmode correlations, which are eigenvector components. The isomorphism allows the thermodynamic constraint on the diagonal heat flux to extend to some degree to the off-diagonal momentum flux. The isomorphism is in force when the cross correlation terms cancel. The thermodynamics constraint of outward heat flux keeps the damped-eigenmode autocorrelation from overpowering the unstable eigenmode autocorrelation. The same combination of autocorrelations appears in the momentum flux so that it remains inward (the direction of quasilinear theory) even with the damped-eigenmode reduction. A set of cross correlation terms breaks the isomorphic structure. When these terms do not cancel one another, as is the case during certain bursts, the momentum flux can change sign and become outward even as the heat flux maintains its outward direction.

The cross correlations reflect the energy transfer dynamics between eigenmodes. While the coupling between eigenmodes is quite complex, it is also sensitive to symmetries such as the conjugate pairing between the unstable and damped eigenmodes. This symmetry causes the cross correlation between the unstable and damped eigenmodes to completely drop out of the momentum and heat fluxes expressions. The cross correlations that survive and are responsible for the effects described above are between the unstable and marginally stable eigenmodes and between the marginally stable and damped eigenmodes. This structure is indicative of a prominent energy channel from the unstable eigenmode to the marginally stable mode as an intermediary and then to damped eigenmode. Other types of intermediate modes also appear to be involved in damped-eigenmode excitation. In gyrokinetic simulations fluctuations with $k_y=0$, whether a zonal flow or the zonal wavenumber of some stable eigenmode, appear to operate as intermediaries in transfer to damped eigenmodes whose wavenumbers do not satisfy $k_y=0$. The possibility that phase-mixing considerations may dictate this energy transfer channel is presently being investigated and will be described elsewhere.

Understanding energy transfer channels between instability and damped eigenmodes is important because this replaces the cascade to high wavenumber of conventional turbulence. The scale invariance of energy transfer in the inertial range of Navier–Stokes turbulence in a powerful or-

ganizing principle that is not applicable to the types of systems discussed in this paper. The transfer instead to a hyperspace of damped-eigenmode manifolds is a complicated and potentially messy story. However, symmetries such as the conjugate symmetry discussed here and processes such as phase mixing in gyrokinetic simulations may provide selection rules that simplify the picture. These kinds of considerations may provide the best path to eventually establishing which damped eigenmodes do not participate significantly in saturation and transport. Such knowledge could potentially be used to create highly efficient reduced models that capture all of the saturation and transport physics by not using computational resources to resolve the eigenmodes that do not matter.

ACKNOWLEDGMENTS

This work was supported by the U.S. Department of Energy through Grant No. DE-FG02-89ER53291.

The authors acknowledge useful discussions with Bill Nevins.

¹P. W. Terry, *Rev. Mod. Phys.* **72**, 109 (2000).

²L.-G. Eriksson, E. Righi, and K.-D. Zastrow, *Plasma Phys. Controlled Fusion* **39**, 27 (1997).

³J. E. Rice, M. Greenwald, I. H. Hutchinson, E. S. Marmor, Y. Takase, S. M. Wolfe, and F. Bombarda, *Nucl. Fusion* **38**, 75 (1998).

⁴J. S. deGrassie, K. H. Burrell, L. R. Baylor, W. Houlberg, and J. Lohr, *Phys. Plasmas* **11**, 4323 (2004).

⁵T. S. Hahm, P. H. Diamond, O. D. Gurcan, and G. Rewoldt, *Phys. Plasmas* **14**, 072302 (2007).

⁶A. G. Peeters, C. Angioni, and D. Strintzi, *Phys. Rev. Lett.* **98**, 265003 (2007).

⁷W. M. Solomon, K. H. Burrell, J. S. deGrassie, R. Budny, R. J. Groebner, J. E. Kinsey, G. J. Kramer, T. C. Luce, M. A. Makowski, D. Mikkelsen, R. Nazikian, C. C. Petty, P. A. Politzer, S. D. Scott, M. A. Van Zeeland, and M. C. Zarnstorff, *Plasma Phys. Controlled Fusion* **49**, B313 (2007).

⁸W. M. Solomon, S. M. Kaye, R. E. Bell, B. P. LeBlanc, J. E. Menard, G. Rewoldt, W. Wang, F. M. Levinton, H. Yuh, and S. Sabbagh, *Phys. Rev. Lett.* **101**, 065004 (2008).

⁹N. Mattor and P. H. Diamond, *Phys. Fluids* **31**, 1180 (1988).

¹⁰B. Coppi and D. Spight, *Phys. Rev. Lett.* **41**, 551 (1978).

¹¹P. W. Terry and R. Gatto, *Phys. Plasmas* **13**, 062309 (2006).

¹²P. W. Terry, D. A. Baver, and S. Gupta, *Phys. Plasmas* **13**, 022307 (2006).

¹³D. R. Hatch, P. W. Terry, W. M. Nevins, and W. Dorland, *Phys. Plasmas* **16**, 022311 (2009).

¹⁴A. Hasegawa and K. Mima, *Phys. Rev. Lett.* **39**, 205 (1977).

¹⁵M. N. Rosenbluth and F. Hinton, *Phys. Rev. Lett.* **80**, 724 (1998).

¹⁶P. W. Terry, R. Gatto, and D. A. Baver, *Phys. Rev. Lett.* **89**, 205001 (2002).

¹⁷J. Lang, S. E. Parker, and Y. Chen, *Phys. Plasmas* **15**, 055907 (2008).

¹⁸P. W. Terry, D. R. Hatch, and J.-H. Kim, *Bull. Am. Phys. Soc.* **53**, 108 (2008).

¹⁹J.-H. Kim and P. W. Terry, *Bull. Am. Phys. Soc.* **53**, 275 (2008).

²⁰D. R. Hatch, P. W. Terry, W. M. Nevins, F. Jenko, and F. Merz, *Bull. Am. Phys. Soc.* **54**, 39 (2009).

²¹G. S. Lee and P. H. Diamond, *Phys. Fluids* **29**, 3291 (1986).

²²C. Holland, P. H. Diamond, S. Champeaux, E. Kim, O. Gurcan, M. N. Rosenbluth, G. R. Tynan, N. Crocker, W. Nevins, and J. Candy, *Nucl. Fusion* **43**, 761 (2003).

²³W. Horton, B. G. Hong, and W. M. Tang, *Phys. Fluids* **31**, 2971 (1988).

²⁴W. M. Nevins, personal communication (2009).